

Stress Corrosion Cracking of Uranium 10 Weight per Cent Molybdenum Alloys in Gaseous and Aqueous Environment.

A. M. Nomine, D. Bedere and D. Miannay

1 - INTRODUCTION. The Uranium, 10 % weight molybdenum alloys possess interesting characteristics : their isotropic, body centered cubic structure can be maintained metastably at room temperature by quenching, their mechanical resistance is high and they have a good corrosion resistance. On the other hand, they are susceptible to stress corrosion cracking (SCC) (1,2,3,4).

A body of results on the SCC in air and water at room temperature and a proposed explanation for this behavior are presented here.

2 - RESULTS. The chemical composition of the alloys studied (3,4) is given in Table I. These alloys were either as cast, or homogeneized and quenched. The ascast alloy showed at the grain size scale an heterogeneity in the molybdenum concentration of the order of 2 weight % and was made of two phases γ and γ' . In the homogeneized state, the γ phase was only present. As the properties depended on the location of the test piece in the ingot, it was distinguished by the letters H (top), B (bottom) and M (middle).

Two types of tests were performed : in the first one namely tensile tests at various strain rates and delayed fracture tests, the three stages of SCC, initiation, propagation and unstable fracture, come into play. In the second one, namely toughness tests in the environment, the two last stages only are to be considered.

Figure 1 shows that in air the endurance limit of the alloy depended on the location and on the heat treatment. However, the results together with those of the literature (1,2) show no correlation between this endurance limit and the grain size or the carbon content. On the fracture surface the SCC zone formed a thumbnail region. From its surface weither the final fracture was a result of unstable fracture or of an increase of the stress above the net resistance of the remaining section was investigated. The results as plotted on figure 2 show that it is not possible to distinguish, as the specimen geometry and the mathematical formulae which were used have their limitations.

Figure 3 shows that in air the mechanical resistance of the alloy is not modified, but that the ductility decreases with the strain rate. The ductility is also a function of the location in the ingot. On the fracture surface, appeared a thumbnail SCC region whose fractional area is plotted on figure 3. Two critical strain rates show up : $4.17 \cdot 10^{-6}$

s^{-1} and $4.17 \cdot 10^{-4} s^{-1}$, the first one corresponding to the nilductility and the second one to the disappearance of SCC. It is remarkable that these same strain rates were also found previously by other authors (1).

Figure 4 shows the toughness measured in air as a function of the loading rate. Although the results are valid according to the ASTM specifications, a SCC propagation can be seen on the fracture surface, more pronounced in the ascast alloy than in the homogenized alloy. This SCC propagation was evidenced as isolated regions with a typical appearance which can probably be attributed to the cristallographic nature of the SCC (3) for the loading rates up to $0,15 \text{ MPa} \sqrt{m} \cdot \Delta A$ less well defined fracture pattern appears at higher loading rate (Fig.5).

Figures 6,7 and 8 show the results concerning the toughness in the environment, in air (relative humidity $HR \approx 50 \%$), in dry air and in water saturated air and in water. It can be seen that : a) cracking begins after an incubation time which decreases when the stress intensity factor increases, b) the crack velocity is quite stress intensity factor independent in the homogenized alloy and almost so in the ascast alloy, which together with the grain size explain why branching is more pronounced in the homogenized material, c) the crack velocity is little affected by the environment : identical in air and water, it tends to increase when the water vapor content increases. It remains close to $1,5 \cdot 10^{-7} \text{ ms}^{-1}$, d) the toughness in the environment K_{ISCC} does not depend on the environment, but depends on the alloy, e) the crack path is transgranular in air and is mixed in water (3,4) and it is independent of the alloy heterogeneity, f) cracking in water is accompanied by the formation of gaz bubbles (3), g) in the ascast alloy, the toughness in air goes from $12 \text{ MPa} \sqrt{m}$ to $18 \text{ MPa} \sqrt{m}$ according to whether precracking was by fatigue or by SCC. It is explained by residual stresses due to the heterogeneity and which were evaluated to be of the order of 190 MPa from the variation of the lattice parameter (3).

3 - INTERPRETATION. Two hypotheses can be put forward in order to explain SCC of the alloy. According to the first one, a thin brittle oxide layer of critical thickness forms and breaks under the applied stress or by the dislocations pile ups or the cracks which are produced in the material due to the epitaxial stresses. According to the second one, the embrittlement is due to the hydrogen which was formed by a surface reaction and was drained in the material by diffusion either in a stress field or by the movement of dislocations. Both hypotheses agree with the experimental findings of the authors (3) and

of Sulsona (2) and with the following interpretations.

In the toughness measurement, the plastic strain rate at the elastic plastic boundary can be written (5) $\dot{\epsilon} = \frac{10Y}{E} \frac{K}{K}$, that is to say $5 \cdot 10^{-4} s^{-1}$ for the critical strain rate of SCC disappearance in the U Mo 10 alloy, exactly the critical strain rate for the SCC disappearance in the tensile tests. Thus, when the strain rate is high enough ($> 5 \cdot 10^{-4} s^{-1}$), the SCC cannot occur : above this rate, the growth of the oxide layer at the surface or the hydrogen pick up in the material are no longer possible. In the first case the epitaxial stresses are difficult to evaluate. In the second one the velocity above which the hydrogen cannot follow the dislocations is (6) $\dot{\epsilon} = \rho D$, which gives for a dislocation density $\rho = 10^7 \text{ cm}^{-2}$, a reasonable value $D = 5 \cdot 10^{-11} \text{ cm}^2 s^{-1}$ for the hydrogen diffusion coefficient. Both hypotheses remain thus valuable for initiation and propagation and explain the incubation time.

The constant value of the crack velocity above K_{ISCC} can be explained by a transport mechanism in the environment or through the reaction products, for instance the transport of O^{2-} , H^+ or OH^- ions (7), or by an adsorption mechanism, as these mechanisms are stress independant. As the reaction rate which leads to the oxide layer formation, varies greatly with the humidity level (7) it seems most likely that the adsorption of water molecules and their dissociation at the surface of the material are the reactions which are rate controlling, the hydrogen being produced in large enough quantity. In water, the dissolution might on contrary play an important role and lead to intergranular cracking. Near K_{ISCC} , the hydrogen transport in the material, highly enhanced by the stress, must be the controlling mechanism.

4. CONCLUSION. SCC in air and water of U Mo 10 alloy seems to be a result of hydrogen embrittlement by the humidity of the environment. The surface oxide plays a role not yet well understood. On the other hand, the plasticity of the material is revealed as a major factor in this cracking. The respective roles of hydrogen and oxygen remain to be found.

BIBLIOGRAPHIE

- (1) C.A.W. PETERSON et R.R. VANDERVOORT, U.C.R.L. 7767, 13 Mars (1964)
- (2) H. SULSONA Ph.D., University of Arizona (1968) 68 - 12 - 922
- (3) A.M. NOMINE, D. BEDERE et D. MIANNAY, à paraître
- (4) N.J. MAGNANI, N.A.C.E. Meeting, Paper n° 58, U.S.A. (1972)
- (5) G.T. HAHN, R.G. HOAGLAND et A.R. ROSENFELD Met. Trans. 2, 2, 537 (1971)
- (6) J. FRIEDEL "Dislocations", Pergamon Press, (1964)
- (7) S. ORMAN Corrosion Science, 12, 1, 35 (1972)

Table I : Alloy characteristics

Alloy	weight composition		heat treatment	metallographic structure	
	Mo, 10 ⁻²	C, 10 ⁻⁶		structure	grain diameter, μm
D. 407 (plate)	9,8	94	as. cast	heterogeneous	100
			homogenised	homogeneous	>200
D. 422 (ingot)	10,6	180	as. cast	heterogeneous	100 . 300
			homogenised	homogeneous	600 . 300
Magnani	9,3	80	quenched		

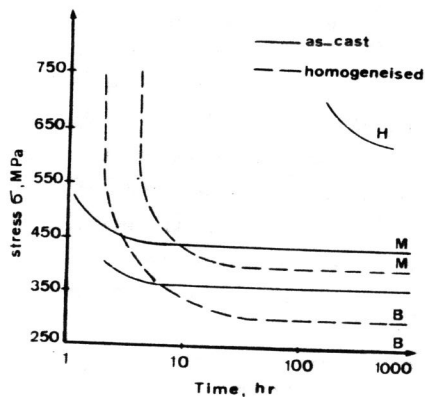
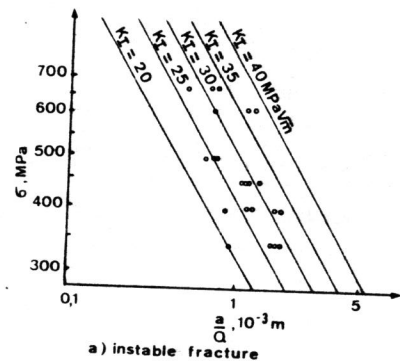
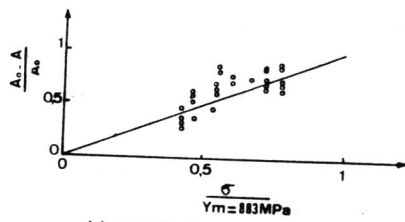


Fig. 1. Delayed failure in air - D. 422 homogenised and as-cast



a) instable fracture



b) normal fracture

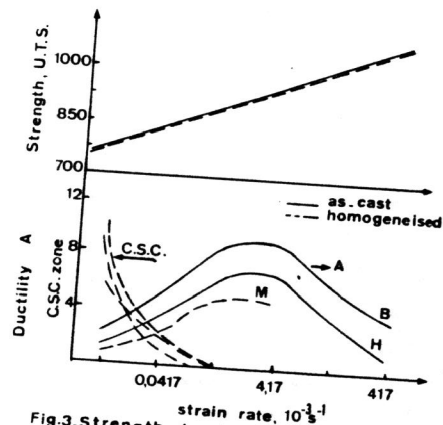


Fig. 3. Strength, ductility and C.S.C extent variations with strain rate - D. 422.

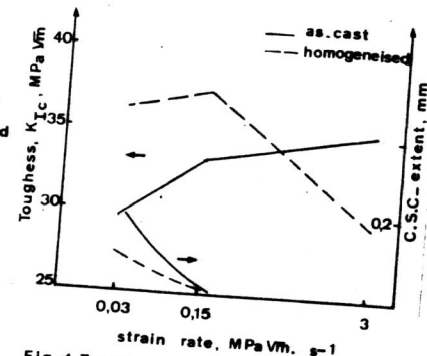


Fig. 4. Toughness and C.S.C extent variations with strain rate - D. 422.

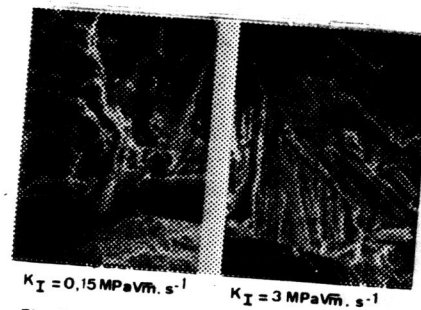


Fig. 5. Fractograph of C.S.C. zone in toughness specimens. D422; homogenised.

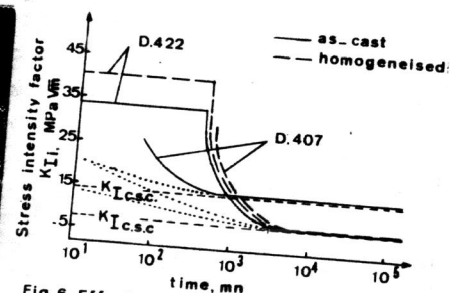


Fig. 6. Effect of stress intensity on the incubation time and the time to fracture in air. HR ≈ 50%

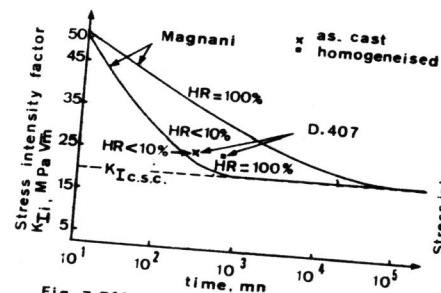


Fig. 7. Effect of stress intensity on the incubation time and the time to fracture in dry air and saturated air.

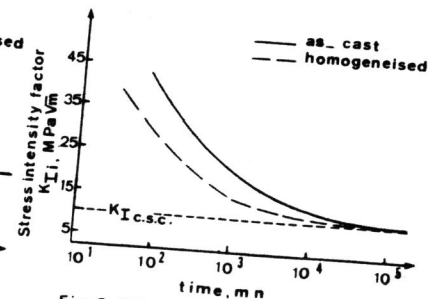


Fig. 8. Effect of stress intensity on the incubation time and the time to fracture in water.